Nonequilibrium solvation for vertical photoemission and photoabsorption processes using the symmetry-adapted cluster–configuration interaction method in the polarizable continuum model

Ryoichi Fukuda,[1,2,a)] Masahiro Ehara,[1,2,b)] Hiroshi Nakatsuji,[2,3,c)] and Roberto Cammi[4,d)]
[1]*Department of Theoretical and Computational Molecular Science, Institute for Molecular Science and Research Center for Computational Science, 38 Nishigo-Naka, Myodaiji, Okazaki 444-8585, Japan*
[2]*Japan Science and Technology Agency CREST, Sanboncho-5, Chiyoda-ku, Tokyo 102-0075, Japan*
[3]*Quantum Chemistry Research Institute, Kyodai Katsura Venture Plaza, 1-36 Goryo Oohara, Nishikyo-ku, Kyoto 615-8245, Japan*
[4]*Dipartmento di Chimica Università di Parma, Viale delle Scienze 17/A, 43100 Parma, Italy*

(Received 13 November 2010; accepted 15 February 2011; published online 14 March 2011)

In this paper, we present the theory and implementation of a nonequilibrium solvation model for the symmetry-adapted cluster (SAC) and symmetry-adapted cluster–configuration interaction (SAC–CI) method in the polarizable continuum model. For nonequilibrium solvation, we adopted the Pekar partition scheme in which solvent charges are divided into dynamical and inertial components. With this nonequilibrium solvation scheme, a vertical transition from an initial state to a final state may be described as follows: the initial state is described by equilibrium solvation, while in the final state, the inertial component remains in the solvation for the initial state; the dynamical component will be calculated self-consistently for the final state. The present method was applied to the vertical photoemission and absorption of s-*trans* acrolein and methylenecyclopropene. The effect of nonequilibrium solvation was significant for a polar solvent. © *2011 American Institute of Physics*. [doi:10.1063/1.3562211]

I. INTRODUCTION

Transitions between electronic states of molecules in solution are important subjects in theoretical and computational chemistry. That is associated with the recent priority issues of molecular science, such as improving the efficiency of light–energy conversion or development of molecular-scale devices. In a previous paper[1] (hereafter we refer to it as paper I), we developed a theory for electronic excitations in solution by generalizing the polarizable continuum model (PCM)[2,3] to molecular solutes described at the level of the symmetry-adapted cluster (SAC) and the SAC–configuration interaction (SAC–CI) methods.[4,5] The basic formulations and the implementations of the SAC/SAC–CI in PCM have been developed in paper I. The analytical energy gradient has already been developed for the SAC/SAC–CI theory, and the equilibrium molecular geometry can be optimized by SAC and SAC–CI in both the ground and excited states.[6] Based on this, an analytical energy gradient for SAC/SAC–CI in PCM has been developed; therefore, the PCM SAC–CI method enables us to study photoabsorption and photoemission processes and chemical reactions of molecules in solution. The SAC–CI method has already been successfully applied to study the photochemistry of various types of systems,[7–9] and therefore, its adaptation to the PCM promises to extend further the applicability of the SAC–CI method. To study the vertical photoabsorption and photoemission processes, however, we have to develop the nonequilibrium solvation model for the SAC/SAC–CI method. This study reports the nonequilibrium solvation model of PCM that has been combined with the SAC and SAC–CI methods.

The concept of nonequilibrium solvation[10–18] has been introduced to describe the solvent polarization in processes involving sudden variation of the solute charge distribution. It takes into account that during the time scale of these processes, not all the degrees of freedoms of the solvent determining the solvent polarization are able to respond to the variations of the solute charge distribution. In the continuum–cavity model for the solvent, the dielectric medium polarization vector field is partitioned into two components; namely, the fast and slow components. The fast component is associated with all the degrees of freedom of the solvent molecules having characteristic times faster than the time scale of the sudden process of the solute, while the slow component collects all the other contributions from the degrees of freedom having slower characteristic times.

In the case of vertical photoabsorption and photoemission processes (whose time scale is about 10^{-15} s), only the electronic degrees of freedom (10^{-15} s) of the solvent are able to determine the fast components of the solvent polarization, which will be equilibrated with the charge distribution of the solute in the final electronic state. All the other degrees of freedom of the solvent molecules (translational, rotational, and vibrational) have much slower relaxation time scales (10^{-12}–10^{-8} s), and they determine the slow component of the solvent polarization, which will remain

a)Electronic mail: fukuda@ims.ac.jp.
b)Electronic mail: ehara@ims.ac.jp.
c)Electronic mail: h.nakatsuji@qcri.or.jp.
d)Electronic mail: chifi@unipr.it.

equilibrated with the charge distribution of the solute in the initial electronic state.

There have been several studies of electronic transitions including the concept of nonequilibrium solvation in quantum mechanical continuum–cavity models, both in the Onsager-like framework and in the PCM-like framework.[19–28] These studies are mainly based on the variational principle of Hartree–Fock self-consistent reaction field (SCF), multiconfiguration SCF, or density functional theory, except for the studies by Christiansen *et al.*, where the nonvariational coupled-cluster response theory was used to evaluate electronic excitation energies.[24] In the present method, we used the free-energy formulation of the SAC/SAC–CI electron correlation theory with a state-specific solvation model. This method can consider any electronic transitions between electronic states that can be treated by the SAC/SAC–CI method.

By combining the present nonequilibrium solvation theory and the PCM SAC/SAC–CI analytical energy gradient method, one can study not only vertical photoabsorptions but also vertical photoemissions in solution. The energy of the emitted photon or the wavelength of luminescence corresponds to the energy difference between route 3 and route 4 in Fig. 1; that is, the energy difference between the ground and excited states in the equilibrium geometry of the excited state. For molecules in solution, we should consider the dynamics of solvent circumstance during the electronic transition between the excited and ground states. The nonequilibrium solvation of PCM has been developed to describe such phenomena.

In this study, the scheme of nonequilibrium solvation was adapted for our recently developed and implemented theory of the SAC/SAC–CI in PCM. For molecules in a vacuum, the transition between route 3 and route 4 is reversible; therefore, we may calculate it as the transition from route 4 to route 3. Namely, we can calculate route 4 by the SAC and calculate route 3 as the SAC–CI state excited from the route 4 SAC state. Obviously, this is a single job for the SAC/SAC–CI calculation. For molecules in solution, the initial and final states are distinguished. The computational strategies for the transition from route 3 to route 4 and for the transition from route 4 to route 3 are different. The final state calculation uses the results of the initial state calculation. Consequently, the transition from route 3 to route 4 requires a two-step process:

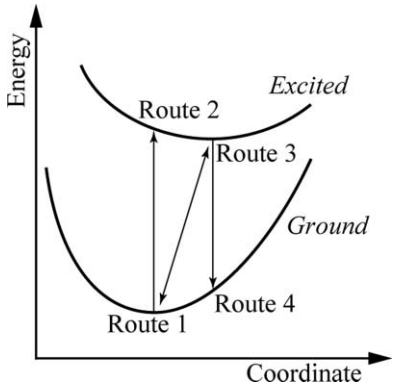

FIG. 1. Computational routes and transitions.

a SAC/SAC–CI calculation for route 3 and a SAC calculation for route 4.

In this paper, we will present the formulation and implementation of nonequilibrium theory for the SAC/SAC–CI in PCM for vertical absorption and vertical emission processes in the framework of the Pekar partition approach. Here, we will explain only the representative electronic transitions, but our formulation and implementation apply generally to any electronic transitions. As typical test cases, vertical transitions of s-*trans* acrolein and methylenecyclopropene have been studied. The effects of nonequilibrium solvation were significant for a polar solvent. The present study would be particularly useful in studying the photoemission process in solution, such as in designing luminescent molecules.

II. NONEQUILIBRIUM SOLVATION MODEL

Within the PCM procedure the dielectric medium polarization is represented in terms of an apparent surface charge (ASC) spread on the cavity surface. To adapt the procedure to the nonequilibrium scheme, one introduces a partition of the ASC into fast and slow components. The operative partition of the ASC can be performed using two alternative, but equivalent, approaches called the Marcus and Pekar approaches. We will follow the Pekar approach, in which the fast and slow components are called dynamical (d) and inertial (in), and denoted as $\mathbf{Q}_m^{\mathrm{d}}$ and $\mathbf{Q}_m^{\mathrm{in}}$, respectively.[3,21,26,27,29,30] They can be determined using the standard PCM equations for the ASC.

The dynamical charge $\mathbf{Q}_x^{\mathrm{d}}$ determined by a generic charge distribution x of the molecular solute may be obtained from the PCM linear system of equations in which the PCM solvent-response matrix is determined using the optical dielectric constant (ε_∞) of the bulk solvent[31] instead of its static dielectric constant ε_0:

$$\mathbf{Q}_x^{\mathrm{d}} = \mathbf{T}(\varepsilon_\infty)\,\mathbf{V}_x, \tag{1}$$

where $\mathbf{T}(\varepsilon_\infty)$ is the response matrix of PCM in the so-called integral equation formulation (IEFPCM)[32] and $\mathbf{V}_x$ is a vector collecting the electrostatic potential produced by the charge distribution x at the location of the ASC. The inertial charge $\mathbf{Q}_y^{\mathrm{in}}$ determined by a generic charge distribution y of the molecular solute may be expressed as a difference between the equilibrium solvation charges $\mathbf{Q}_y$ and dynamical charges $\mathbf{Q}_y^{\mathrm{d}}$ associated with the charge distribution y:

$$\mathbf{Q}_y^{\mathrm{in}} = \mathbf{Q}_y - \mathbf{Q}_y^{\mathrm{d}}, \tag{2}$$

with

$$\mathbf{Q}_y = \mathbf{T}(\varepsilon_0)\,\mathbf{V}_y, \tag{3}$$

where $\mathbf{T}(\varepsilon_0)$ is the IEFPCM response matrix, which is evaluated with the static dielectric constant of the solvent, and $\mathbf{V}_y$ is a vector collecting the electrostatic potential produced by the charge distribution y at the location of the ASC.

III. PCM SAC–CI VERTICAL EMISSION WITH NONEQUILIBRIUM SOLVATION

Let us consider the case of a vertical photoemission process from an excited state |SAC–CI, eq⟩, which we assume is

equilibrated with all the degrees of freedom of the solvent, to the ground state $|\text{SAC, neq}\rangle$, which will be in a nonequilibrium solvation regime:

$$|\text{SAC–CI, eq}\rangle \xrightarrow{-h\nu} |\text{SAC, neq}\rangle. \tag{4}$$

The total (equilibrium) polarization charges for the initial state $|\text{SAC–CI, eq}\rangle$ will be given by

$$\mathbf{Q}_{|\text{SAC–CI,eq}\rangle} = \mathbf{Q}^{\text{d}}_{|\text{SAC–CI,eq}\rangle} + \mathbf{Q}^{\text{in}}_{|\text{SAC–CI,eq}\rangle}, \tag{5}$$

while in the final ground state $|\text{SAC, neq}\rangle$, the total (nonequilibrium) polarization charges will be given by the sum of the dynamical charges $\mathbf{Q}^{\text{d}}_{|\text{SAC,neq}\rangle}$ and the inertial charges, $\mathbf{Q}^{\text{in}}_{|\text{SAC–CI,eq}\rangle}$, namely

$$\mathbf{Q}_{|\text{SAC,neq}\rangle} = \mathbf{Q}^{\text{d}}_{|\text{SAC,neq}\rangle} + \mathbf{Q}^{\text{in}}_{|\text{SAC–CI,eq}\rangle}. \tag{6}$$

The scheme to evaluate these polarization charges is arranged by reflecting the specific functional form of the electron-correlated SAC and SAC–CI wavefunctions, which involve a suitable Hartree–Fock reference state. Because of this specific form, the electrostatic potential vector for the SAC or SAC–CI state is partitioned into a contribution of the Hartree–Fock reference state and that of the electron correlation. This electrostatic potential determines the PCM polarization charges; therefore, the polarization charges have the appropriate partition.

For the excited state $|\text{SAC–CI, eq}\rangle$, the electrostatic potential vector $\mathbf{V}_{|\text{SAC–CI,eq}\rangle}$ is given by

$$\mathbf{V}_{|\text{SAC–CI,eq}\rangle} = \mathbf{V}_{\text{HF,eq}} + \Delta\mathbf{V}_{\text{SAC–CI,eq}}, \tag{7}$$

where $\mathbf{V}_{\text{HF,eq}}$ is the contribution of the Hartree–Fock reference state $|\text{HF, eq}\rangle$ and $\Delta\mathbf{V}_{\text{SAC–CI,eq}}$ is the SAC–CI contribution. The components of the PCM SAC–CI polarization charges will be partitioned as follows:

$$\mathbf{Q}_{|\text{SAC–CI,eq}\rangle} = \mathbf{Q}_{\text{HF,eq}} + \Delta\mathbf{Q}_{\text{SAC–CI,eq}}, \tag{8}$$

$$\mathbf{Q}^{\text{d}}_{|\text{SAC–CI,eq}\rangle} = \mathbf{Q}^{\text{d}}_{\text{HF,eq}} + \Delta\mathbf{Q}^{\text{d}}_{\text{SAC–CI,eq}}, \tag{9}$$

$$\mathbf{Q}^{\text{in}}_{|\text{SAC–CI,eq}\rangle} = \mathbf{Q}^{\text{in}}_{\text{HF,eq}} + \Delta\mathbf{Q}^{\text{in}}_{\text{SAC–CI,eq}}. \tag{10}$$

In a similar way, the electrostatic potential vector $\mathbf{V}_{|\text{SAC,neq}\rangle}$ for the nonequilibrium ground state is given by

$$\mathbf{V}_{|\text{SAC,neq}\rangle} = \mathbf{V}_{\text{HF,neq}} + \Delta\mathbf{V}_{\text{SAC}}, \tag{11}$$

where $\mathbf{V}_{\text{HF,neq}}$ is the contribution of the nonequilibrium Hartree–Fock reference state $|\text{HF, neq}\rangle$ and $\Delta\mathbf{V}_{\text{SAC}}$ is the contribution of the nonequilibrium SAC state. Then the total nonequilibrium PCM SAC charges will be given by Eq. (6) and

$$\mathbf{Q}^{\text{d}}_{|\text{SAC,neq}\rangle} = \mathbf{Q}^{\text{d}}_{\text{HF,neq}} + \Delta\mathbf{Q}^{\text{d}}_{\text{SAC,neq}}. \tag{12}$$

The computation method for determining the equilibrium excited state $|\text{SAC–CI, eq}\rangle$ has been described in paper I. In Secs. III A and III B, we will describe how to determine the nonequilibrium PCM SAC state $|\text{SAC, neq}\rangle = \exp\left(S_{\text{neq}}\right)|\text{HF, neq}\rangle$.

A. PCM Hartree–Fock equation for nonequilibrium solvation

We first consider the nonequilibrium Hartree–Fock reference state $|\text{HF, neq}\rangle$ associated with the vertical emission process from the excited state $|\text{SAC–CI, eq}\rangle$ to the ground state $|\text{SAC, neq}\rangle$. Within the Pekar formalism,[21,30] the nonequilibrium Hartree–Fock state $|\text{HF, neq}\rangle$ can be obtained by the stationary condition of the free-energy functional $\mathcal{G}_{\text{HF,neq}}$, which is written as follows:[3]

$$\begin{aligned}\mathcal{G}_{\text{HF,neq}} = {} & \left\langle \text{HF, neq}\left|H^0\right|\text{HF, neq}\right\rangle + \tfrac{1}{2}\mathbf{Q}^{\text{d}}_{\text{HF,neq}}\cdot\mathbf{V}_{\text{HF,neq}} \\ & + \tfrac{1}{2}\mathbf{Q}^{\text{d}}_{\text{HF,neq}}\cdot\mathbf{V}_{\text{nuc}} + \tfrac{1}{2}\mathbf{Q}^{\text{d}}_{\text{nuc}}\cdot\mathbf{V}_{\text{HF,neq}} \\ & + (\mathbf{Q}^{\text{in}}_{\text{nuc}} + \mathbf{Q}^{\text{in}}_{|\text{SAC–CI,eq}\rangle})\cdot\mathbf{V}_{\text{HF,neq}} + \tfrac{1}{2}\mathbf{Q}^{\text{d}}_{\text{nuc}}\cdot\mathbf{V}_{\text{nuc}} \\ & - \tfrac{1}{2}\mathbf{Q}^{\text{in}}_{\text{nuc}}\cdot\mathbf{V}_{|\text{SAC–CI,eq}\rangle} + \tfrac{1}{2}\mathbf{Q}^{\text{in}}_{|\text{SAC–CI,eq}\rangle}\cdot\mathbf{V}_{\text{nuc}} \\ & - \tfrac{1}{2}\mathbf{Q}^{\text{in}}_{|\text{SAC–CI,eq}\rangle}\cdot\mathbf{V}_{|\text{SAC–CI,eq}\rangle} + \tfrac{1}{2}\mathbf{Q}^{\text{in}}_{\text{nuc}}\cdot\mathbf{V}_{\text{nuc}},\end{aligned} \tag{13}$$

where

$$\mathbf{Q}^{\text{d}}_{\text{HF,neq}} = \left\langle \text{HF, neq}\left|\mathbf{Q}^{\text{d}}\right|\text{HF, neq}\right\rangle, \tag{14}$$

$$\mathbf{V}_{\text{HF,neq}} = \langle \text{HF, neq}\,|\mathbf{V}|\,\text{HF, neq}\rangle\,. \tag{15}$$

Here, we have introduced, for convenience, the d/in partition of the polarization charges because of the electrostatic potential $\mathbf{V}_{\text{nuc}}$ that is generated by the nuclear charges of the solute, namely

$$\mathbf{Q}_{\text{nuc}} = \mathbf{Q}^{\text{d}}_{\text{nuc}} + \mathbf{Q}^{\text{in}}_{\text{nuc}}. \tag{16}$$

In an N-electron system with spin-orbitals, which are expanded over a set of atomic orbital (AO) bases $\{\chi_\mu,\ \chi_\nu,\ \ldots\}$, $\mathcal{G}_{\text{HF,neq}}$ may be written as

$$\begin{aligned}\mathcal{G}_{\text{HF,neq}} = {} & \sum_{\mu\nu} P^{\text{HF,neq}}_{\mu\nu}\left[h_{\mu\nu} + \tfrac{1}{2}\left(j^{\text{d}}_{\mu\nu} + y^{\text{d}}_{\mu\nu}\right) + j^{\text{in}}_{\mu\nu} + X^{\text{in}}_{\mu\nu}\right] \\ & + \tfrac{1}{2}\sum_{\mu\nu\lambda\sigma} P^{\text{HF,neq}}_{\mu\nu}P^{\text{HF,neq}}_{\lambda\sigma}\left[\langle\mu\lambda\,\|\nu\sigma\,\rangle + \mathcal{B}^{\text{d}}_{\mu\nu.\lambda\sigma}\right] \\ & + \tfrac{1}{2}\mathbf{Q}^{\text{d}}_{\text{nuc}}\cdot\mathbf{V}_{\text{nuc}} - \tfrac{1}{2}\mathbf{Q}^{\text{in}}_{\text{nuc}}\cdot\mathbf{V}_{|\text{SAC–CI,eq}\rangle} + \tfrac{1}{2}\mathbf{Q}^{\text{in}}_{|\text{SAC–CI,eq}\rangle} \\ & \times\mathbf{V}_{\text{nuc}} - \tfrac{1}{2}\mathbf{Q}^{\text{in}}_{|\text{SAC–CI,eq}\rangle}\cdot\mathbf{V}_{|\text{SAC–CI,eq}\rangle} + \tfrac{1}{2}\mathbf{Q}^{\text{in}}_{\text{nuc}}\cdot\mathbf{V}_{\text{nuc}},\end{aligned} \tag{17}$$

where $h_{\mu\nu}$ is the one-electron part of the Hamiltonian in AO basis, $\langle\mu\lambda\,\|\nu\sigma\,\rangle$ is an antisymmetrized combination of the two-electron repulsion integrals (ERIs), and $P^{\text{HF,neq}}_{\mu\nu}$ denotes the elements of the Hartree–Fock density matrix. The matrix elements $j^{\text{d/in}}_{\mu\nu}$, $y^{\text{d}}_{\mu\nu}$, $X^{\text{in}}_{\mu\nu}$, and $\mathcal{B}^{\text{d}}_{\mu\nu.\lambda\sigma}$ represent the solute–solvent interactions within the PCM Fock operator. More specifically, the one-particle AO integrals $j^{\text{d/in}}_{\mu\nu}$ and $y^{\text{d}}_{\mu\nu}$ represent the interaction with the nuclear component of the ASCs. The pseudo-two-electron integrals $X^{\text{in}}_{\mu\nu}$ and $\mathcal{B}^{\text{d}}_{\mu\nu.\lambda\sigma}$ represent the interactions with the electronic component of the ASCs.

The interaction integrals may be expressed in the following form:

$$j^{\mathrm{d}}_{\mu\nu} = \mathbf{V}_{\mu\nu} \cdot \mathbf{Q}^{\mathrm{d}}_{\mathrm{nuc}}, \tag{18}$$

$$y^{\mathrm{d}}_{\mu\nu} = \mathbf{V}_{\mathrm{nuc}} \cdot \mathbf{Q}^{\mathrm{d}}_{\mu\nu}, \tag{19}$$

$$j^{\mathrm{in}}_{\mu\nu} = \mathbf{V}_{\mu\nu} \cdot \mathbf{Q}^{\mathrm{in}}_{\mathrm{nuc}}, \tag{20}$$

$$X^{\mathrm{in}}_{\mu\nu} = \mathbf{V}_{\mu\nu} \cdot \mathbf{Q}^{\mathrm{in}}_{|\mathrm{SAC-CI,eq}\rangle}, \tag{21}$$

$$\mathcal{B}^{\mathrm{d}}_{\mu\nu.\lambda\sigma} = \mathbf{V}_{\mu\nu} \cdot \mathbf{Q}^{\mathrm{d}}_{\lambda\sigma}. \tag{22}$$

The dynamical charges in the AO basis are given by

$$\mathbf{Q}^{\mathrm{d}}_{\lambda\sigma} = \mathbf{T}\left(\varepsilon_{\infty}\right)\mathbf{V}_{\lambda\sigma}, \tag{23}$$

where $\mathbf{V}_{\lambda\sigma}$ is a vector collecting the AO integrals of the electrostatic potential operator associated with the elementary charge distributions spanned by the AO basis $\chi^{*}_{\lambda}(\mathbf{r})\,\chi_{\sigma}(\mathbf{r})$.

Requiring that $\mathcal{G}_{\mathrm{HF,neq}}$ be stationary with respect to the variation of MO coefficients, we obtain the PCM Hartree–Fock equations for nonequilibrium solvation as

$$\sum_{\nu}\left(f^{\mathrm{PCM,neq}}_{\mu\nu} - \varepsilon_{p} S_{\mu\nu}\right) c_{\nu p} = 0, \tag{24}$$

where $S_{\mu\nu}$ and $f^{\mathrm{PCM,neq}}_{\mu\nu}$ are the elements of the overlap and of the PCM Fock matrices in the AO basis, respectively and ε_{p} and $c_{\nu p}$ are the orbital energy and the expansion coefficients of the pth MO, respectively. The PCM Fock matrix elements are given by

$$f^{\mathrm{PCM,neq}}_{\mu\nu} = h_{\mu\nu} + j^{\mathrm{d}}_{\mu\nu} + j^{\mathrm{in}}_{\mu\nu} + X^{\mathrm{in}}_{\mu\nu} + G_{\mu\nu}\left(\mathbf{P}^{\mathrm{HF,neq}}\right) + X^{\mathrm{d}}_{\mu\nu}\left(\mathbf{P}^{\mathrm{HF,neq}}\right), \tag{25}$$

where

$$G_{\mu\nu}\left(\mathbf{P}^{\mathrm{HF,neq}}\right) = \sum_{\lambda\sigma} P^{\mathrm{HF,neq}}_{\lambda\sigma}\,\langle \mu\lambda \,\|\nu\sigma\,\rangle \tag{26}$$

are the matrix elements of the effective Coulomb-exchange two-electron operator and

$$j^{\mathrm{in}}_{\mu\nu} + X^{\mathrm{in}}_{\mu\nu} = \mathbf{V}_{\mu\nu} \cdot \left(\mathbf{Q}^{\mathrm{in}}_{\mathrm{nuc}} + \mathbf{Q}^{\mathrm{in}}_{|\mathrm{SAC-CI,neq}\rangle}\right), \tag{27}$$

$$j^{\mathrm{d}}_{\mu\nu} = \mathbf{V}_{\mu\nu} \cdot \mathbf{Q}^{\mathrm{d}}_{\mathrm{nuc}}, \tag{28}$$

$$X^{\mathrm{d}}_{\mu\nu}\left(\mathbf{P}^{\mathrm{HF,neq}}\right) = \sum_{\lambda\sigma} P^{\mathrm{HF,neq}}_{\lambda\sigma}\mathcal{B}^{\mathrm{d}}_{\mu\nu.\lambda\sigma} = \mathbf{V}_{\mu\nu}\cdot\mathbf{Q}^{\mathrm{d}}_{|\mathrm{HF,neq}\rangle}. \tag{29}$$

B. PCM SAC nonequilibrium free-energy functional and equations

The ground state PCM SAC wavefunction is defined by Eq. (30) using the Hartree–Fock wavefunction of the solute molecule as the reference state:

$$|\Psi_{\mathrm{SAC,\,neq}}\rangle = \exp\left(S_{\mathrm{neq}}\right)|\mathrm{HF,\,neq}\rangle = \exp\left(\sum_{I} C_{I} S^{\dagger}_{I}\right)|\mathrm{HF,\,neq}\rangle, \tag{30}$$

$$\langle \Lambda',\ \mathrm{neq}| = \langle \mathrm{HF,\,neq}|\sum_{L} Z^{\mathrm{SAC}}_{L} S_{L}, \tag{31}$$

where $|\mathrm{HF,\,neq}\rangle$ is obtained as the solution of the PCM Hartree–Fock equations in the nonequilibrium regime of Eq. (24).

The nonequilibrium PCM SAC free-energy functional may be written as

$$L^{\mathrm{PCM}}_{\mathrm{SAC,neq}} = \langle \Lambda | H^{\mathrm{HF,neq}}_{N} | \Psi_{\mathrm{SAC,neq}}\rangle - \langle \Lambda' | \Psi_{\mathrm{SAC,neq}}\rangle \times \langle 0 | H^{\mathrm{HF,neq}}_{N} | \Psi_{\mathrm{SAC,neq}}\rangle + \tfrac{1}{2}\Delta\mathbf{Q}^{\mathrm{d}}_{\mathrm{SAC,neq}} \cdot \Delta\mathbf{V}_{\mathrm{SAC,neq}}, \tag{32}$$

where $H^{\mathrm{HF,neq}}_{N}$ is the Hamiltonian for the solute in the presence of the Hartree–Fock polarization charges for the nonequilibrium solvation regime and $\Delta\mathbf{Q}^{\mathrm{d}}_{\mathrm{SAC,neq}}$ and $\Delta\mathbf{V}_{\mathrm{SAC,neq}}$ are the SAC contribution of the nonequilibrium polarization charge and the electrostatic potential of the molecular solute, respectively. The nonequilibrium Hamiltonian $H^{\mathrm{HF,neq}}_{N}$ is given by

$$H^{\mathrm{HF,neq}}_{N} = H_{N} + (\mathbf{Q}^{\mathrm{d}}_{|\mathrm{HF,neq}\rangle} + \mathbf{Q}^{\mathrm{in}}_{|\mathrm{SAC-CI,eq}\rangle} + \mathbf{Q}_{\mathrm{nuc}})\mathbf{V}_{N}, \tag{33}$$

where H_{N} is the normal ordered Hamiltonian of the isolated molecule. A vector correcting the Hartree–Fock polarization charges $\mathbf{Q}^{\mathrm{d}}_{|\mathrm{HF,neq}\rangle}$ is defined by Eq. (14), where the Hartree–Fock contribution is limited to the dynamical component of the polarization response of the medium. The remaining electronic component $\mathbf{Q}^{\mathrm{in}}_{|\mathrm{SAC-CI,eq}\rangle}$ is a vector collecting the inertial polarization charges of the excited state. The operator $\mathbf{V}_{N}$ is a vector collecting the normal ordered electrostatic potential operator at the position of the polarization charges. The SAC expectation values $\Delta\mathbf{Q}^{\mathrm{d}}_{\mathrm{SAC,neq}}$ and $\Delta\mathbf{V}_{\mathrm{SAC,neq}}$ in the last term of $L^{\mathrm{PCM}}_{\mathrm{SAC,neq}}$ in Eq. (32) may be written as

$$\Delta\mathbf{Q}^{\mathrm{d}}_{\mathrm{SAC,neq}} = \langle \Lambda,\,\mathrm{neq}|Q^{\mathrm{d}}_{N}|\Psi_{\mathrm{SAC,neq}}\rangle - \langle \Lambda',\,\mathrm{neq}|\Psi_{\mathrm{SAC,neq}}.\rangle \times \langle \mathrm{HF,\,neq}|Q^{\mathrm{d}}_{N}|\Psi_{\mathrm{SAC,neq}}\rangle, \tag{34}$$

$$\Delta\mathbf{V}^{\mathrm{d}}_{\mathrm{SAC,neq}} = \langle \Lambda,\,\mathrm{neq}|V^{\mathrm{d}}_{N}|\Psi_{\mathrm{SAC,neq}}\rangle - \langle \Lambda',\,\mathrm{neq}|\Psi_{\mathrm{SAC,neq}}.\rangle \times \langle \mathrm{HF,\,neq}|V^{\mathrm{d}}_{N}|\Psi_{\mathrm{SAC,neq}}\rangle, \tag{35}$$

where Q^{d}_{N} and V^{d}_{N} are, respectively, the normal ordered form of the dynamical apparent charge operator and of the electrostatic potential operator

$$Q^{\mathrm{d}}_{N} = \mathbf{Q}^{\mathrm{d}} - \mathbf{Q}^{\mathrm{d}}_{|\mathrm{HF,neq}\rangle}, \tag{36}$$

$$V^{\mathrm{d}}_{N} = \mathbf{V}^{\mathrm{d}} - \mathbf{V}^{\mathrm{d}}_{|\mathrm{HF,neq}\rangle}. \tag{37}$$

The equations for the SAC wavefunction (right vector) $|\Psi_{\mathrm{SAC,neq}}\rangle$ are given by

$$\langle \mathrm{HF,\ neq}|S_L(H_N^{\mathrm{PCM,neq}} - \Delta E_{\mathrm{SAC,neq}}^{\mathrm{PCM}})|\Psi_{\mathrm{SAC,neq}}\rangle = 0, \tag{38}$$

where $H_N^{\mathrm{PCM,neq}}$ is the PCM SAC Hamiltonian for the solute and $\Delta E_{\mathrm{SAC,neq}}^{\mathrm{PCM}}$ is the corresponding correlation energy. Equation (38) corresponds to the left projection of the Schrödinger equation of the SAC wavefunction

$$H_N^{\mathrm{PCM,neq}}|\Psi_{\mathrm{SAC,neq}}\rangle = \Delta E_{\mathrm{SAC,neq}}^{\mathrm{PCM}}|\Psi_{\mathrm{SAC,neq}}\rangle \tag{39}$$

with

$$H_N^{\mathrm{PCM,neq}} = H_N^{\mathrm{HF,neq}} + \Delta\mathbf{Q}_{\mathrm{SAC,neq}}\cdot\mathbf{V}_N = H_N^{\mathrm{HF,neq}} + (\mathbf{Q}_{\mathrm{SAC,neq}}^{\mathrm{d}} + \mathbf{Q}_{|\mathrm{SAC-CI,eq}\rangle}^{\mathrm{in}} + \Delta\mathbf{Q}_{\mathrm{SAC,neq}}^{\mathrm{d}})\cdot\mathbf{V}_N, \tag{40}$$

$$\Delta E_{\mathrm{SAC,neq}}^{\mathrm{PCM}} = \langle \mathrm{HF,\ neq}|H_N^{\mathrm{PCM,neq}}|\Psi_{\mathrm{SAC,neq}}\rangle. \tag{41}$$

The Z-SAC equations for the left vector $\langle\Lambda', \mathrm{neq}|$ are given by

$$\begin{aligned}&\langle\Lambda, \mathrm{neq}|H_N^{\mathrm{PCM,neq}}S_L^\dagger|\Psi_{\mathrm{SAC,neq}}\rangle - \langle\Lambda', \mathrm{neq}|S_L^\dagger|\Psi_{\mathrm{SAC,neq}}\rangle\\ &-\langle \mathrm{HF,\ neq}|H_N^{\mathrm{PCM,neq}}|\Psi_{\mathrm{SAC,neq}}\rangle + \langle\Lambda', \mathrm{neq}|\Psi_{\mathrm{SAC,neq}}\rangle\\ &-\langle \mathrm{HF,\ neq}|H_N^{\mathrm{PCM,neq}}S_L^\dagger|\Psi_{\mathrm{SAC,neq}}\rangle = 0.\end{aligned} \tag{42}$$

IV. PCM SAC–CI VERTICAL ABSORPTION WITH NONEQUILIBRIUM SOLVATION

Next, we consider the case of a vertical photoabsorption process from an equilibrium ground state $|\mathrm{SAC,\ eq}\rangle$ to a nonequilibrium excited state $|\mathrm{SAC–CI,\ neq}\rangle$:

$$|\mathrm{SAC,\ eq}\rangle \xrightarrow{+h\nu} |\mathrm{SAC–CI,\ neq}\rangle. \tag{43}$$

The total (equilibrium) polarization charges for the initial state $|\mathrm{SAC,\ eq}\rangle$ will be given by

$$\mathbf{Q}_{|\mathrm{SAC,eq}\rangle} = \mathbf{Q}_{|\mathrm{SAC,eq}\rangle}^{\mathrm{d}} + \mathbf{Q}_{|\mathrm{SAC,eq}\rangle}^{\mathrm{in}}, \tag{44}$$

while in the final excited state $|\mathrm{SAC–CI,\ neq}\rangle$, the total (nonequilibrium) polarization charges will be given by

$$\mathbf{Q}_{|\mathrm{SAC-CI,neq}\rangle} = \mathbf{Q}_{|\mathrm{SAC-CI,neq}\rangle}^{\mathrm{d}} + \mathbf{Q}_{|\mathrm{SAC,eq}\rangle}^{\mathrm{in}}. \tag{45}$$

For the equilibrium ground state $|\mathrm{SAC,\ eq}\rangle$, the electrostatic potential vector $\mathbf{V}_{|\mathrm{SAC,eq}\rangle}$ is given by

$$\mathbf{V}_{|\mathrm{SAC,eq}\rangle} = \mathbf{V}_{\mathrm{HF,eq}} + \Delta\mathbf{V}_{\mathrm{SAC,eq}}, \tag{46}$$

where $\mathbf{V}_{\mathrm{HF,eq}}$ is the contribution of the Hartree–Fock reference state $|\mathrm{HF,\ eq}\rangle$ and $\Delta\mathbf{V}_{\mathrm{SAC,eq}}$ is the SAC contribution. The components of the PCM SAC polarization charges will be given as follows:

$$\mathbf{Q}_{|\mathrm{SAC,eq}\rangle} = \mathbf{Q}_{\mathrm{HF,eq}} + \Delta\mathbf{Q}_{\mathrm{SAC,eq}}, \tag{47}$$

$$\mathbf{Q}_{|\mathrm{SAC,eq}\rangle}^{\mathrm{d}} = \mathbf{Q}_{\mathrm{HF,eq}}^{\mathrm{d}} + \Delta\mathbf{Q}_{\mathrm{SAC,eq}}^{\mathrm{d}}, \tag{48}$$

$$\mathbf{Q}_{|\mathrm{SAC,eq}\rangle}^{\mathrm{in}} = \mathbf{Q}_{\mathrm{HF,eq}}^{\mathrm{in}} + \Delta\mathbf{Q}_{\mathrm{SAC,eq}}^{\mathrm{in}}. \tag{49}$$

In a similar way, the electrostatic potential vector for the nonequilibrium excited state is given by

$$\mathbf{V}_{|\mathrm{SAC-CI,neq}\rangle} = \mathbf{V}_{\mathrm{HF,neq}} + \Delta\mathbf{V}_{\mathrm{SAC-CI,neq}}, \tag{50}$$

where $\mathbf{V}_{\mathrm{HF,neq}}$ is the contribution of the nonequilibrium Hartree–Fock reference state and $\Delta\mathbf{V}_{\mathrm{SAC-CI,neq}}$ is the contribution of the nonequilibrium SAC–CI state. Then the total nonequilibrium PCM SAC–CI charges will be given by Eq. (45) and

$$\mathbf{Q}_{|\mathrm{SAC-CI,neq}\rangle}^{\mathrm{d}} = \mathbf{Q}_{\mathrm{HF,neq}}^{\mathrm{d}} + \Delta\mathbf{Q}_{\mathrm{SAC-CI,neq}}^{\mathrm{d}}. \tag{51}$$

The computation method for the equilibrium ground state $|\mathrm{SAC,\ eq}\rangle$ has been described in paper I. The nonequilibrium excited state $|\mathrm{SAC–CI,\ neq}\rangle$ is determined in a similar way to that for $|\mathrm{SAC,\ neq}\rangle$ described in Sec. III.

A. PCM Hartree–Fock equation for the nonequilibrium reference state

Here we consider the nonequilibrium Hartree–Fock reference state $|\mathrm{HF,\ neq}\rangle$ associated with the vertical absorption process from the ground state $|\mathrm{SAC,\ eq}\rangle$ to the excited state $|\mathrm{SAC–CI,\ neq}\rangle$ within the Pekar formalism.[21,30] The free-energy functional is given as[3]

$$\begin{aligned}\mathcal{G}_{\mathrm{HF,neq}} =& \langle \mathrm{HF,\ neq}|H^0|\mathrm{HF,\ neq}\rangle + \tfrac{1}{2}\mathbf{Q}_{\mathrm{HF,neq}}^{\mathrm{d}}\cdot\mathbf{V}_{\mathrm{HF,neq}}\\ &+ \tfrac{1}{2}\mathbf{Q}_{\mathrm{HF,neq}}^{\mathrm{d}}\cdot\mathbf{V}_{\mathrm{nuc}} + \tfrac{1}{2}\mathbf{Q}_{\mathrm{nuc}}^{\mathrm{d}}\cdot\mathbf{V}_{\mathrm{HF,neq}}\\ &+ (\mathbf{Q}_{\mathrm{nuc}}^{\mathrm{in}} + \mathbf{Q}_{|\mathrm{SAC,eq}\rangle}^{\mathrm{in}})\cdot\mathbf{V}_{\mathrm{HF,neq}} + \tfrac{1}{2}\mathbf{Q}_{\mathrm{nuc}}^{\mathrm{d}}\cdot\mathbf{V}_{\mathrm{nuc}}\\ &- \tfrac{1}{2}\mathbf{Q}_{\mathrm{nuc}}^{\mathrm{in}}\cdot\mathbf{V}_{|\mathrm{SAC,eq}\rangle} + \tfrac{1}{2}\mathbf{Q}_{|\mathrm{SAC,eq}\rangle}^{\mathrm{in}}\cdot\mathbf{V}_{\mathrm{nuc}}\\ &- \tfrac{1}{2}\mathbf{Q}_{|\mathrm{SAC,eq}\rangle}^{\mathrm{in}}\cdot\mathbf{V}_{|\mathrm{SAC,eq}\rangle} + \tfrac{1}{2}\mathbf{Q}_{\mathrm{nuc}}^{\mathrm{in}}\cdot\mathbf{V}_{\mathrm{nuc}}.\end{aligned} \tag{52}$$

This can be obtained from Eq. (13) by replacing $\mathbf{Q}_{|\mathrm{SAC-CI,eq}\rangle}^{\mathrm{in}}$ and $\mathbf{V}_{|\mathrm{SAC-CI,eq}\rangle}$ by $|\mathrm{SAC,\ eq}\rangle$ correspondences. The AO representation of $\mathcal{G}_{\mathrm{HF,neq}}$ may be written as

$$\begin{aligned}\mathcal{G}_{\mathrm{HF,neq}} =& \sum_{\mu\nu} P_{\mu\nu}^{\mathrm{HF,neq}}[h_{\mu\nu} + \tfrac{1}{2}(j_{\mu\nu}^{\mathrm{d}} + y_{\mu\nu}^{\mathrm{d}}) + j_{\mu\nu}^{\mathrm{in}} + X_{\mu\nu}^{\mathrm{in}}]\\ &+ \tfrac{1}{2}\sum_{\mu\nu\lambda\sigma} P_{\mu\nu}^{\mathrm{HF,neq}}P_{\lambda\sigma}^{\mathrm{HF,neq}}[\langle\mu\lambda\|\nu\sigma.\rangle + \mathcal{B}_{\mu\nu.\lambda\sigma}^{\mathrm{d}}]\\ &+ \tfrac{1}{2}\mathbf{Q}_{\mathrm{nuc}}^{\mathrm{d}}\cdot\mathbf{V}_{\mathrm{nuc}} - \tfrac{1}{2}\mathbf{Q}_{\mathrm{nuc}}^{\mathrm{in}}\cdot\mathbf{V}_{|\mathrm{SAC,eq}\rangle} + \tfrac{1}{2}\mathbf{Q}_{|\mathrm{SAC,eq}\rangle}^{\mathrm{in}}\cdot\mathbf{V}_{\mathrm{nuc}}\\ &- \tfrac{1}{2}\mathbf{Q}_{|\mathrm{SAC,eq}\rangle}^{\mathrm{in}}\cdot\mathbf{V}_{|\mathrm{SAC,eq}\rangle} + \tfrac{1}{2}\mathbf{Q}_{\mathrm{nuc}}^{\mathrm{in}}\cdot\mathbf{V}_{\mathrm{nuc}},\end{aligned} \tag{53}$$

where

$$X_{\mu\nu}^{\mathrm{in}} = \mathbf{V}_{\mu\nu}\cdot\mathbf{Q}_{|\mathrm{SAC,eq}\rangle}^{\mathrm{in}}, \tag{54}$$

and other matrix elements have already been defined in Sec. III. The MO coefficients that define the reference state

$|\mathrm{HF, neq}\rangle$ will be obtained by the PCM Hartree–Fock equations derived by the stationary conditions for $\mathcal{G}_{\mathrm{HF,neq}}$ of Eq. (53).

B. PCM SAC–CI nonequilibrium free-energy functional and equations

The PCM SAC–CI vectors for the nonequilibrium (pth) excited state are defined by

$$|\Psi_{\mathrm{SAC-CI,neq}}\rangle = R^p|\Psi_{\mathrm{SAC,neq}}\rangle = \sum_M d_M^p R_M^\dagger|\Psi_{\mathrm{SAC,neq}}\rangle, \tag{55}$$

$$\langle\Psi^L_{\mathrm{SAC-CI,neq}}| = \langle\mathrm{HF, neq}|L^p = \langle\mathrm{HF, neq}|\sum_M d_M^{Lp} R_M, \tag{56}$$

$$\langle\Lambda''| = \sum_K Z_K^{\mathrm{SAC-CI}}\langle\mathrm{HF, neq}|S_K, \tag{57}$$

where $|\mathrm{HF, neq}\rangle$ is the nonequilibrium Hartree–Fock state of the molecular solute and $|\mathrm{SAC, neq}\rangle$ is the SAC wavefunction that satisfies the SAC equation

$$\langle\mathrm{HF, neq}|S_K H_N^{\mathrm{HF,neq}}|\Psi_{\mathrm{SAC,neq}}\rangle - \langle\mathrm{HF, neq}|S_K|\Psi_{\mathrm{SAC,neq}}\rangle \times \langle\mathrm{HF, neq}|H_N^{\mathrm{HF,neq}}|\Psi_{\mathrm{SAC,neq}}\rangle = 0, \tag{58}$$

where $H_N^{\mathrm{HF,neq}}$ is the Hamiltonian given by

$$H_N^{\mathrm{HF,neq}} = H_N + (\mathbf{Q}^{\mathrm{d}}_{\mathrm{HF,neq}} + \mathbf{Q}^{\mathrm{in}}_{|\mathrm{SAC,eq}\rangle} + \mathbf{Q}_{\mathrm{nuc}})\mathbf{V}_N. \tag{59}$$

The PCM SAC–CI nonequilibrium free-energy functional may be written as

$$\begin{aligned} L^{\mathrm{PCM}}_{\mathrm{SAC-CI,neq}} = {} & \langle\Psi^L_{\mathrm{SAC-CI,neq}}|H_N^{\mathrm{HF,neq}}|\Psi_{\mathrm{SAC-CI,neq}}\rangle \\ & - \langle\Lambda''|H_N^{\mathrm{HF,neq}}|\Psi_{\mathrm{SAC,neq}}\rangle \\ & - \langle\Lambda''|\Psi_{\mathrm{SAC,neq}}\cdot\rangle\langle\mathrm{HF, neq}|H_N^{\mathrm{HF,neq}}|\Psi_{\mathrm{SAC,neq}}\rangle \\ & + \tfrac{1}{2}\Delta\mathbf{Q}^d_{\mathrm{SAC-CI,neq}}\Delta\mathbf{V}_{\mathrm{SAC-CI,neq}}, \end{aligned} \tag{60}$$

where $\Delta\mathbf{Q}^{\mathrm{d}}_{\mathrm{SAC-CI,neq}}$ and $\Delta\mathbf{V}_{\mathrm{SAC-CI,neq}}$ are, respectively, the SAC–CI expectation value of the dynamical polarization charges and the electrostatic potential operator

$$\Delta\mathbf{Q}^{\mathrm{d}}_{\mathrm{SAC-CI,neq}} = \langle\Psi^L_{\mathrm{SAC-CI,neq}}|Q^{\mathrm{d}}_N|\Psi_{\mathrm{SAC-CI,neq}}\rangle, \tag{61}$$

$$\Delta\mathbf{V}_{\mathrm{SAC-CI,neq}} = \langle\Psi^L_{\mathrm{SAC-CI,neq}}|V^{\mathrm{d}}_N|\Psi_{\mathrm{SAC-CI,neq}}\rangle, \tag{62}$$

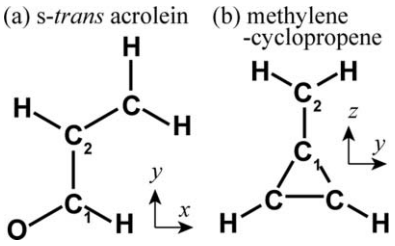

FIG. 2. Molecular coordinate system of (a) s-*trans* acrolein and (b) methylenecyclopropene.

with

$$Q^{\mathrm{d}}_N = \mathbf{Q}^{\mathrm{d}} - \mathbf{Q}^{\mathrm{d}}_{\mathrm{HF,neq}}. \tag{63}$$

The PCM SAC–CI equations may be obtained from the stationary condition of the free-energy functional $L^{\mathrm{PCM}}_{\mathrm{SAC-CI,neq}}$. The stationarity of $L^{\mathrm{PCM}}_{\mathrm{SAC-CI,neq}}$ with respect to the R^p and L^p amplitudes leads, respectively, to the left and right projections of the Schrödinger equation of the SAC–CI wavefunction

$$H_N^{\mathrm{PCM,neq}}|\Psi_{\mathrm{SAC-CI,neq}}\rangle = \Delta E^{\mathrm{PCM}}_{\mathrm{SAC-CI,neq}}|\Psi_{\mathrm{SAC-CI,neq}}\rangle, \tag{64}$$

$$\langle\Psi^L_{\mathrm{SAC-CI,neq}}|H_N^{\mathrm{PCM,neq}} = \langle\Psi^L_{\mathrm{SAC-CI,neq}}|\Delta E^{\mathrm{PCM}}_{\mathrm{SAC-CI,neq}}, \tag{65}$$

where the PCM SAC–CI energy is given by

$$\Delta E^{\mathrm{PCM}}_{\mathrm{SAC-CI,neq}} = \langle\Psi^L_{\mathrm{SAC-CI,neq}}|H_N^{\mathrm{PCM,neq}}|\Psi_{\mathrm{SAC-CI,neq}}\rangle, \tag{66}$$

and $H_N^{\mathrm{PCM,neq}}$ is the PCM SAC–CI Hamiltonian for the solute for the excited state of interest:

$$H_N^{\mathrm{PCM,neq}} = H_N^{\mathrm{HF,neq}} + \Delta\mathbf{Q}^d_{\mathrm{SAC-CI,neq}}\mathbf{V}_N. \tag{67}$$

V. TEST CALCULATIONS

As typical test cases of solvatochromic shifts of vertical transition energies, we chose the lowest transition of s-*trans* acrolein (C_3H_4O) and methylenecyclopropene (C_4H_4) in nonpolar and polar solvents because their equilibrium molecular geometries have already been studied by the PCM SAC/SAC–CI method.[1] For s-*trans* acrolein both the ground and the lowest excited states ($n \rightarrow \pi^*$) have planar structures. The lowest excited states ($\pi \rightarrow \pi^*$) of methylenecyclopropene is not planar; however, here we used the optimized geometry restricted to a planar conformation. The optimized geometries by the PCM SAC/SAC–CI with cc-pVDZ basis[33] have been reported in paper I. Using these geometries,

TABLE I. Vertical emission energy (VEE) and its solvent shift (shift) for s-*trans* acrolein.

	SAC–CI nonequilibrium		SAC–CI equilibrium		Experiment[a]
Solvent	VEE (eV)	Shift (eV)	VEE (eV)	Shift (eV)	VEE (eV)
Vacuum	2.915	0.000	2.915	0.000	
n-hexane	2.896	−0.019	2.895	−0.020	3.31, 3.16, 3.00
Aqueous	2.774	−0.141	2.854	−0.061	

[a]Observed fluorescence in 2-methyl-THF at 77 K (Ref. 36).

TABLE II. Vertical absorption energy (VAE) and its solvent shift (shift) for s-*trans* acrolein.

	SAC–CI nonequilibrium		SAC–CI equilibrium		Experiment	
Solvent	VAE (eV)	Shift (eV)	VAE (eV)	Shift (eV)	VAE (eV)	Shift (eV)
Vacuum	3.838	0.000	3.838	0.000	3.75[a], 3.69[b]	
n-hexane	3.829	− 0.009	3.829	− 0.009		
Aqueous	3.913	+ 0.075	3.809	− 0.029		+ 0.2[c]

[a]Reference 36.
[b]Reference 37.
[c]References 38–41.

transition energies were calculated with the cc-pVDZ basis, except where noted otherwise. The coordinate systems of molecule used in the present calculations are shown in Fig. 2. For s-*trans* acrolein, the molecule was set in the *x*-*y* plane where the C_1C_2 bond was set to the *y*-axis. For methylenecyclopropene, the molecule was set in the *y*-*z* plane where C_1C_2 bond was set to the *z*-axis.

The perturbation-selection technique was not used in the present calculations. The PCM SAC–CI program was implemented based on the latest version of the direct SAC–CI program[34] combined with GAUSSIAN 09.[35] The default parameters of IEFPCM in GAUSSIAN 09 were used.

A. s-*trans* acrolein

The vertical emission energies are shown in Table I using the nonequilibrium and equilibrium solvation schemes. The fluorescence spectrum of s-*trans* acrolein in 2-methyl-THF at 77 K has been reported in Ref. 36. The observed spectrum has poorly resolved peaks at 375, 392, and 413 nm (3.31, 3.16, and 3.00 eV). The position of the peak maximum is 3.16 or 3.00 eV; thus, the present calculation seems to underestimate the emission energy by about 0.1–0.3 eV.

The solvent effect in *n*-hexane is small, and the effect of nonequilibrium solvation is negligible. The effect of water is significant; the calculated solvent shift was −0.141 eV (22 nm) by the nonequilibrium solvation model. Nonequilibrium solvation is very important for aqueous solutions. The equilibrium solvation model greatly underestimated the solvent effect because the equilibrium model overestimated the relaxation of the degree of freedom of the solvent.

The vertical absorption energies are shown in Table II using the nonequilibrium and equilibrium solvation schemes. The solvent shift for *n*-hexane is small, and the effect of nonequilibrium solvation is negligible. The solvent shift for water is significant; moreover, the direction of the solvent shift is different between the equilibrium and the nonequilibrium solvation schemes. If we use equilibrium solvation, the calculated shift was negative and the result contradicted the experimental findings. Nonequilibrium solvation reproduced the observed higher energy shift (blueshift) in aqueous solution. The present PCM SAC–CI calculation with nonequilibrium solvation still underestimated the observed solvent shift by more than 0.1 eV. This underestimation would be attributed to the lack of explicit hydrogen bonds.

Table III shows the dipole moments in the ground and the $n \rightarrow \pi^*$ excited states in vacuum with the ground and the excited state geometries. The dipole moment in the ground state is larger than that in the excited state. For the vertical absorption process, the ground state is stabilized by solvation. Consequently, the vertical absorption energy shows blueshift in polar solvent. For the vertical emission process, the final (ground) state has larger dipole moment and this state is destabilized by the nonequilibrium solvation, where the inertial component of solvation charges remains in the solvation for the less-polar initial state. As a result, the vertical emission energy shows lower energy shift (redshift) in polar solvent.

The results of nonequilibrium calculations with larger basis, aug-cc-pVDZ (Ref. 42) and cc-pVTZ (Ref. 33), are shown in Table IV. Here we used the same molecular geometry as the cc-pVDZ calculations. We also calculated the vertical excitation (absorption) energy of the lowest $\pi \rightarrow \pi^*$ state because the experimental data are available. For the absorption energy of lowest $n \rightarrow \pi^*$ transition, basis set effects were small in vacuum and in *n*-hexane; they were about 0.01 eV or less. Using larger basis sets, the excitation energy in aqueous solution was increased. Consequently, the calculated solvent shift became large with using larger basis sets. The solute polarization can be properly described by flexible basis set.

The basis set dependence was large for the lowest $\pi \rightarrow \pi^*$ state; particularly, the effect of diffuse function was significant. This indicates the mixing of Rydberg character in this state. The solvent shifts calculated with augmented diffuse functions were small in comparison with the results without diffuse functions. The excited state is confined in a solvent cavity and is destabilized. This would suggest that the interaction between the tail of solute wavefunction and

TABLE III. Dipole moment (debye) of s-*trans* acrolein in vacuum with the ground and the lowest $n \rightarrow \pi^*$ state geometries. The dipole moment $|d|$ and its Cartesian components are shown.

	Component			
State	*x*	*y*	*z*	$\|d\|$
Ground state geometry				
Ground	1.961	1.938	0.000	2.757
$n \rightarrow \pi^*$	0.959	0.096	0.000	0.964
$n \rightarrow \pi^*$ state geometry				
Ground	2.329	2.315	0.000	3.284
$n \rightarrow \pi^*$	1.116	0.462	0.000	1.208

TABLE IV. Basis set dependence of vertical excitation energy (VAE) and vertical emission energy (VEE) for s-*trans* acrolein with nonequilibrium solvation model. The solvent shifts from vacuum are given in parentheses (in eV).

	SAC–CI nonequilibrium			
Solvent	cc-pVDZ	aug-cc-pVDZ	cc-pVTZ	Experiment
		VAE ($n \rightarrow \pi^*$)		
Vacuum	3.838	3.832	3.849	3.75,[a] 3.69[b]
n-hexane	3.829 (−0.009)	3.826 (−0.006)	3.833 (−0.016)	
Aqueous	3.913 (+0.075)	3.939 (+0107)	3.948 (+0.099)	(+0.2)[c]
		VAE ($\pi \rightarrow \pi^*$)		
Vacuum	7.187	6.749	6.941	6.41,[d] 6.42[e]
n-hexane	7.098 (−0.089)	6.716 (−0.033)	6.851 (−0.090)	
Aqueous	6.992 (−0.195)	6.611 (−0.138)	6.733 (−0.208)	(−0.4)[f]
		VEE ($n \rightarrow \pi^*$)		
Vacuum	2.915	2.969	2.960	
n-hexane	2.896 (−0.019)	2.962 (−0.007)	2.949 (−0.011)	3.31, 3,16, 3.00[g]
Aqueous	2.774 (−0.141)	2.844 (−0.125)	2.827 (−0.133)	

[a]Reference 36.
[b]Reference 37.
[c]References 38–41.
[d]Reference 43.
[e]Reference 44.
[f]References 38–41, 43, and 44.
[g]Observed fluorescence in 2-methyl-THF at 77 K (Ref. 36).

solvent molecules are significant. The PCM may be insufficient to describe this kind of interaction; therefore, our calculation underestimated the solvent shift of excitation energy. Similar discussion has been given by the quantum mechanics/molecular mechanics (QM/MM) calculations,[37,45] in which the excitation energy strongly depends on the number of explicit solvent molecules. Furthermore, we need to discuss the radii of molecular cavity of the PCM for using diffuse basis function. However, it is beyond the purpose of this study.

For the vertical emission energy, larger basis sets increase the emission energies about 0.05 eV and the agreement with experiment was improved. The basis set dependences are similar both in vacuum and in solution; therefore, the basis set dependence of solvent shift is small.

B. Methylenecyclopropene

The vertical emission energies are shown in Table V using the nonequilibrium and equilibrium solvation schemes. We restricted the excited state geometry to being planar; therefore, the present results cannot be compared to experimental findings. In the $\pi \rightarrow \pi^*$ excited state, the molecule becomes twisted conformation and intersystem crossing might be possible. Investigating such a possibility is beyond the purpose of the present study. Here, we are only interested in "sudden polarization"[47] of this molecule: the significant difference in the dipole moment in the ground and the first excited states. Thus, we used the optimized geometry restricted to being planar.

The solvent effect in *n*-hexane is about −0.03 eV and the effect of nonequilibrium solvation is negligible. The effect of water is significant; the calculated solvent shift was −0.28 eV (22 nm) by the nonequilibrium solvation model. Nonequilibrium solvation is very important for aqueous solutions. The relaxation of solvent degrees of freedom in the final ground state considered by the equilibrium solvation model is significant; that effect is about 0.22 eV because the directions of the dipole moment for this molecule is different between the ground and the first excited states.

The transition energies for the vertical absorption process are shown in Table VI using the nonequilibrium and equilibrium solvation schemes. The solvent shift for *n*-hexane is

TABLE V. Vertical emission energy (VEE) and its solvent shift (shift) for methylenecyclopropene.

	SAC–CI nonequilibrium		SAC–CI equilibrium	
Solvent	VEE (eV)	Shift (eV)	VEE (eV)	Shift (eV)
Vacuum	2.165	0.000	2.165	0.000
n-hexane	2.136	− 0.029	2.135	− 0.030
Aqueous	1.885	− 0.280	2.102	− 0.063

TABLE VI. Vertical absorption energy (VAE) and its solvent shift (shift) for methylenecyclopropene.

	SAC–CI nonequilibrium		SAC–CI equilibrium		Experiment
Solvent	VAE (eV)	Shift (eV)	VAE (eV)	Shift (eV)	VAE (eV)
Vacuum	4.734	0.000	4.734	0.000	
n-hexane	4.669	−0.065	4.670	−0.064	4.01[a]
Aqueous	4.832	+0.098	4.572	−0.162	4.49[b]

[a]In *n*-pentane −78°C (Ref. 46).
[b]In methanol −78°C (Ref. 46).

TABLE VII. Dipole moment (debye) of methylenecyclopropene in vacuum with the ground and $\pi \rightarrow \pi^*$ excited state geometries. The dipole moment $|d|$ and its Cartesian components are shown.

State	Component x	y	z	$\|d\|$
Ground state geometry				
Ground	0.000	0.000	− 1.859	1.859
$\pi \rightarrow \pi^*$	0.000	0.000	1.980	1.980
$\pi \rightarrow \pi^*$ state geometry				
Ground	0.000	0.000	− 2.716	2.716
$\pi \rightarrow \pi^*$	0.000	0.000	1.192	1.192

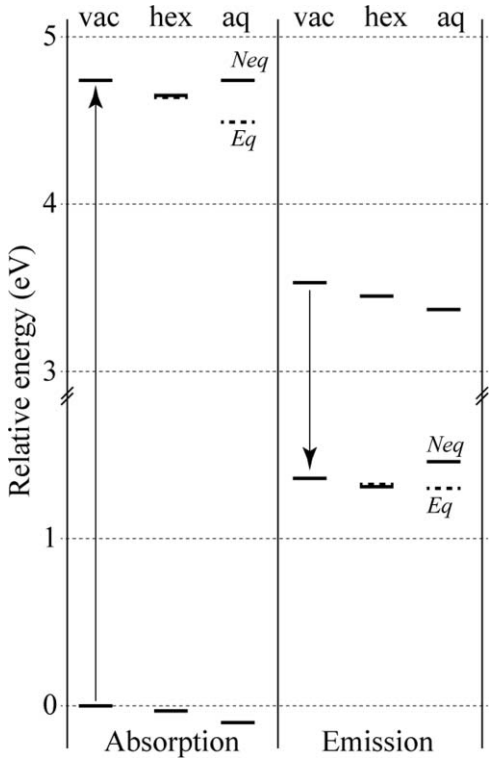

FIG. 3. Relative energies of methylenecyclopropene in the ground and first excited states, where the ground state geometry was used for absorption and the excited state geometry with a planar constraint was used for emission. Solid horizontal lines denote nonequilibrium solvation results and broken lines denote equilibrium solvation results.

not negligible, although the nonequilibrium and equilibrium solvation schemes gave almost the same transition energies. A large positive solvent shift was obtained for water in the nonequilibrium solvation model. The relaxation of solvent considered by the equilibrium model is very large; the energy shift is about 0.26 eV. Such a large relaxation effect of solvent degree of freedom was attributed to the sudden polarization.

Table VII shows the dipole moments in the ground and the $\pi \rightarrow \pi^*$ excited states in vacuum with the ground and the excited state geometries. The direction of the dipole moment is alternated by the electronic excitation. This drastic change of molecular dipole moment causes significant solvent effects.

A diagram of the relative energies of methylenecyclopropene is shown in Fig. 3. We took the energy standard as the ground state of absorption (the ground state geometry) in vacuum. In this figure, vac, hex, and aq denote the results in vacuum, in *n*-hexane, and in water, respectively. The energy of the initial states (the ground state for absorption and the excited state for emission) is stabilized by solvent. The final state energies were also stabilized in the equilibrium solvation. However, for the nonequilibrium solvation, the final state energies were destabilized by polar solvent because of the repulsive interaction between the solute dipole moment and the inertial part of the solvent charges.

The results of nonequilibrium calculations with larger basis sets are shown in Table VIII. Here we used the same molecular geometry as the cc-pVDZ calculations. In particular, the effect of diffuse function was significant; it was about 0.25 eV. The agreement between calculation and experiment was improved by adding diffuse functions. For the vertical emission energy, basis set dependence was small.

TABLE VIII. Basis set dependence of vertical excitation energy (VAE) and vertical emission energy (VEE) for methylenecyclopropene with nonequilibrium solvation model. The solvent shifts from vacuum are given in parentheses (in eV).

Solvent	SAC–CI nonequilibrium cc-pVDZ	aug-cc-pVDZ	cc-pVTZ	Experiment
VAE ($\pi \rightarrow \pi^*$)				
Vacuum	4.734	4.471	4.635	
n-hexane	4.669 (−0.065)	4.412 (−0.059)	4.567 (−0.068)	4.01[a]
Aqueous	4.832 (+0.098)	4.601 (+0.130)	4.747 (+0.112)	4.49[b]
VEE ($n \rightarrow \pi^*$)				
Vacuum	2.165	2.123	2.160	
n-hexane	2.136 (−0.065)	2.104 (−0.108)	2.130 (−0.030)	
Aqueous	1.885 (−0.280)	1.856 (−0.356)	1.864 (−0.296)	

[a]In *n*-pentane −78°C (Ref. 46).
[b]In methanol −78°C (Ref. 46).

The present results for the vertical absorption energy with the nonequilibrium solvation scheme are almost the same as our previous results reported in paper I, in which the nonequilibrium solvation charges in the initial ground state were approximated by the Hartree–Fock contribution only. In particular, the ΔSAC contributions in Eqs. (46)–(49) were neglected in the results reported in paper I. This approximation may work if the polarization charges in the ground state are well described by the Hartree–Fock level. This assumption is valid for the present test case of vertical absorption. For vertical emission, however, the Hartree–Fock state is not an approximation for the initial state. Neglecting the ΔSAC–CI contributions in Eqs. (7)–(10) is inadequate.

VI. CONCLUSIONS

In this paper, we presented the theory and implementation of a nonequilibrium solvation model for the SAC/SAC–CI method in PCM to describe the vertical photoabsorption and emission processes of molecules in solution. In the PCM, nonequilibrium solvation is modeled by the partition of solvent charges into fast and slow components. In this study, we adopted the Pekar partition, which divides the solvation contribution into dynamical (fast) and inertial (slow) parts. In this scheme, the nonequilibrium solvation of a transition from an initial state to a final state may be described as follows: the initial state is described by the usual equilibrium solvation that was described in the previous paper, while in the final state, the inertial part remains in the solvation for the initial state; the dynamical part will change into the solvation for the final state. In the PCM SAC/SAC–CI method, the solvent affects both the SAC/SAC–CI amplitudes and the reference Hartree–Fock state; therefore, our formulation changes the PCM Hartree–Fock equation for the final state, in which the contributions from the initial SAC/SAC–CI wavefunction appear.

The nonequilibrium solvation model was implemented in the recently developed PCM SAC–CI program incorporated with the GAUSSIAN development version. The initial and final states were calculated as a multistep job in GAUSSIAN. We have already implemented the analytical energy gradients of excited states in the solvent with the PCM SAC–CI method, and the present study gives a scheme to calculate vertical transition energies. Then, one can calculate the vertical photoemission process in solution using the PCM SAC/SAC–CI method.

Test calculations for s-*trans* acrolein and methylenecyclopropene were presented. The effect of nonequilibrium solvation is significant for a polar solvent, particularly for methylenecyclopropene. The present scheme would be particularly useful in the study of photoemission processes. For absorption, solute–solvent interaction using the Hartree–Fock state is usually a good approximation for the initial state. Under such an approximation, the nonequilibrium scheme becomes quite simple. For emission, however, the initial state should be the SAC–CI correlated wavefunction. Thus, the present scheme is essential. The PCM SAC/SAC–CI will provide a useful method for studying and designing light-emitting compounds by *ab initio* calculations.

ACKNOWLEDGMENTS

R.C. thanks the Italian MIUR "Ministero dell'Istruzione, Universitae Ricerca" for financial support (PRIN2007). The authors acknowledge support from a grant-in-aid for Scientific Research from the Japan Society for the Promotion of Science (JSPS) and the Ministry of Education, Culture, Sports, Science and Technology (MEXT) Japan and the Next Generation Supercomputing Project. The computations were performed using the Research Center for Computational Science, Okazaki, Japan.

APPENDIX: COMPUTATIONAL STEPS

Evaluation of the nonequilibrium vertical emission energy involves the following steps:

1. The PCM SAC–CI energy calculation for the equilibrium excited state |SAC–CI, eq⟩; these steps are essentially the same as the method described in paper I, but terms necessary for the next steps are saved.
   - 1-1. The PCM Hartree–Fock calculation for |HF, eq⟩ is performed. At the end, compute and save the inertial charges $\mathbf{Q}^{\text{in}}_{\text{HF,eq}}$ and $\mathbf{Q}^{\text{in}}_{\text{nuc}}$ and the potentials $\mathbf{V}^{\text{in}}_{\text{HF,eq}}$.
   - 1-2. The PCM SAC equations (equilibrium) for |SAC, eq⟩ are solved.
   - 1-3. The PCM SAC–CI equations (equilibrium) are solved for |SAC–CI, eq⟩. At the end, compute the inertial charges $\Delta\mathbf{Q}^{\text{in}}_{\text{SAC–CI,eq}}$ and the potentials $\Delta\mathbf{V}^{\text{in}}_{\text{SAC–CI,eq}}$ and incrementally add them to $\mathbf{Q}^{\text{in}}_{\text{HF,eq}}$ and $\mathbf{V}^{\text{in}}_{\text{HF,eq}}$. The resulting total inertial charges $\mathbf{Q}^{\text{in}}_{\text{SAC–CI,eq}}$ and total potential $\mathbf{V}^{\text{in}}_{\text{SAC–CI,eq}}$ are saved.
2. The PCM SAC energy calculation for the nonequilibrium ground state |SAC, neq⟩.
   - 2-1. The PCM Hartree–Fock nonequilibrium state equations (24) are solved for |HF, neq⟩.
   - 2-2. The PCM SAC equations (38) are solved for |SAC, neq⟩.

The programs have been implemented for GAUSSIAN 09; |SAC–CI, eq⟩ and |SAC, neq⟩ are calculates as a multistep job. The information is transferred by a common checkpoint file.

[1] R. Cammi, R. Fukuda, M. Ehara, and H. Nakatsuji, J. Chem. Phys. **133**, 024104 (2010).
[2] S. Miertuš, E. Scrocco, and J. Tomasi, Chem. Phys. **55**, 117 (1981).
[3] J. Tomasi, B. Mennucci, and R. Cammi, Chem. Rev. **105**, 2999 (2005).
[4] H. Nakatsuji and K. Hirao, Chem. Phys. Lett. **47**, 569 (1977); J. Chem. Phys. **68**, 2053 (1978).
[5] H. Nakatsuji, Chem. Phys. Lett. **59**, 362 (1978); *ibid.* **67**, 329 (1979); *ibid.* **67**, 334 (1979).
[6] T. Nakajima and H. Nakatsuji, Chem. Phys. Lett. **280**, 79 (1997); Chem. Phys. **242**, 177 (1999); K. Toyota, M. Ehara, and H. Nakatsuji, Chem. Phys. Lett. **356**, 1 (2002); K. Toyota, M. Ishida, M. Ehara, M. J. Frisch, and H. Nakatsuji, Chem. Phys. Lett. **367**, 730 (2003).
[7] H. Nakatsuji, Bull. Chem. Soc. Jpn. **78**, 1705 (2005); J. Hasegawa and H. Nakatsuji, in *Radiation Induced Molecular Phenomena in Nucleic Acid: A Comprehensive Theoretical and Experimental Analysis*, edited by M. Shukla and J. Leszczynsk (Springer, New York, 2008), Chap. 4, pp. 93–124; M. Ehara, J. Hasegawa, and H. Nakatsuji, in *Theory and Applications of Computational Chemistry: The First 40 Years, A Volume of Technical and Historical Perspectives*, edited by C. E. Dykstra, G. Frenking, K. S. Kim, and G. E. Scuseria (Elsevier, Oxford, 2005), pp. 1099–1141.

[8]P. Poolmee, M. Ehara, S. Hannongbua, and H. Nakatsuji, Polymer **46**, 6474 (2005); B. Saha, M. Ehara, and H. Nakatsuji, J. Phys. Chem. A **111**, 5473 (2007); M. Promkatkaew, S. Suramitr, T. K. Karpkird, S. Namuangruk, M. Ehara, and S. Hannongbua, J. Chem. Phys. **131**, 224306 (2009); R. Fukuda, M. Ehara, and H. Nakatsuji, *ibid*. **133**, 144316 (2010).
[9]A. K. Das, J. Hasegawa, T. Miyahara, M. Ehara, and H. Nakatsuji, J. Comput. Chem. **24**, 1421 (2003); K. Fujimoto, J. Hasegawa, S. Hayashi, S. Kato, and H. Nakatsuji, Chem. Phys. Lett. **414**, 239 (2005); N. Nakatani, J. Hasegawa, and H. Nakatsuji, J. Am. Chem. Soc. **129**, 8756 (2007).
[10]R. Marcus, J. Chem. Phys. **24**, 966 (1956).
[11]J. Jortner, Mol. Phys. **5**, 257 (1962).
[12]J. Ulstrup, *Charge TransferPprocesses in Condensed Media* (Springer-Verlag, Berlin, 1979).
[13]G. Van Der Zwan and J. T. Hynes, J. Phys. Chem. **89**, 4181 (1985).
[14]H. J. Kim and J. T. Hynes, J. Chem. Phys. **93**, 5194 (1990); **93**, 5211 (1990).
[15]M. D. Newton and H. L. Friedman, J. Chem. Phys. **88**, 4460 (1988).
[16]M. V. Basilevsky and G. E. Chudionov, Chem. Phys. **157**, 327 (1991); M. V. Basilevsky, G. E. Chudionov, and D. V. Napolov, J. Phys. Chem. **97**, 3270 (1993).
[17]D. G. Truhlar, G. K. Schenter, and B. C. Garrett, J. Chem. Phys. **98**, 5756 (1993); C. Cramer and D. G. Truhlar, Chem. Rev. **99**, 2161 (1999).
[18]A. Nitzan, *Chemical Dynamics in Condensed Phases* (Oxford University Press, Oxford, 2006).
[19]R. Bonaccorsi, R. Cimiraglia, and J. Tomasi, J. Comput. Chem. **4**, 567 (1983); R. Bonaccorsi, R. Cimiraglia, and J. Tomasi, Chem. Phys. Lett. **99**, 77 (1983).
[20]M. A. Aguilar, F. J. Olivares del Valle, and J. Tomasi, J. Chem. Phys. **98**, 7375 (1993).
[21]R. Cammi and J. Tomasi, Int. J. Quantum Chem., Symp. **29**, 465 (1995).
[22]K. V. Mikkelsen, A. Cesar, H. Ågren, and H. J. Aa. Jensen, J. Chem. Phys. **103**, 9010 (1995).
[23]B. Mennucci, R. Cammi, and J. Tomasi, J. Chem. Phys. **109**, 2798 (1998).
[24]O. Christiansen and K. V. Mikkelsen, J. Chem. Phys. **110**, 8348 (1999).
[25]M. Cossi and V. Barone, J. Phys. Chem. A **104**, 10614 (2000); J. Chem. Phys. **115**, 4708 (2001).
[26]R. Cammi, L. Frediani, B. Mennucci, J. Tomasi, K. Ruud, and K. V. Mikkelsen, J. Chem. Phys. **117**, 13 (2002).
[27]R. Cammi, S. Corni, B. Mennucci, and J. Tomasi, J. Chem. Phys. **122**, 104513 (2005).
[28]S. Corni, R. Cammi, B. Mennucci, and J. Tomasi, J. Chem. Phys. **123**, 134512 (2005).
[29]M. Caricato, B. Mennucci, J. Tomasi, F. Ingrosso, R. Cammi, S. Corni, and G. Scalmani, J. Chem. Phys. **124**, 124520 (2006).
[30]C. Cappelli, S. Corni, R. Cammi, B. Mennucci, and J. Tomasi, J. Chem. Phys. **113**, 11270 (2000).
[31]The optical dielectric constant is related by the Maxwell relation to the refractive index, n, of the bulk solvent as $\varepsilon_\infty = n^2$.
[32]E. Cances, B. Mennucci, and J. Tomasi, J. Chem. Phys. **107**, 3032 (1997); E. Cances and B. Mennucci, J. Math. Chem. **23**, 309 (1998); B. Mennucci, E. Cances, and J. Tomasi, J. Phys. Chem. B **101**, 10506 (1997).
[33]T. H. Dunning, Jr., J. Chem. Phys. **90**, 1007 (1989).
[34]R. Fukuda and H. Nakatsuji, J. Chem. Phys. **128**, 094105 (2008).
[35]M. J. Frisch, G. W. Trucks, H. B. Schlegel *et al.*, GAUSSIAN 09, Revision B.01 Gaussian, Inc., Wallingford, CT, 2010.
[36]R. S. Becker, K. Inuzuka, and J. King, J. Chem. Phys. **52**, 5164 (1970).
[37]K. Aidas, A. Møgelhøj, E. J. K. Nilsson, M. S. Johnson, K. V. Mikkelsen, O. Christiansen, P. Söderhjelm, and J. Kongsted, J. Chem. Phys. **128**, 194503 (2008).
[38]G. Mackinney and O. Temmer, J. Am. Chem. Soc. **70**, 3586 (1948).
[39]K. Inuzuka, Bull. Chem. Soc. Jpn. **33**, 678 (1960).
[40]A. F. Moskvin, O. P. Yablonskii, and L. F. Bondar, Theor. Exp. Chem. **2**, 469 (1966).
[41]A. M. D. Lee, J. D. Coe, S. Ullrich, M.-L. Ho, S.-J. Lee, B.-M. Cheng, M. Z. Zgierski, I.-C. Chen, T. J. Martínez, and A. Stolow, J. Phys. Chem. A **111**, 11948 (2007).
[42]R. A. Kendall, T. H. Dunning, Jr., and R. J. Harrison, J. Chem. Phys. **96**, 6796 (1992).
[43]A. D. Walsh, Trans. Faraday Soc. **41**, 498 (1945).
[44]J. M. Hollas, Spectrochim. Acta. **19**, 1425 (1963).
[45]K. Sneskov, E. Matito, J. Kongsted, and O. Christiansen, J. Chem. Theory Comput. **6**, 839 (2010).
[46]S. W. Staley and T. D. Norden, J. Am. Chem. Soc. **106**, 3699 (1984).
[47]R. P. Johnson and M. W. Schmidt, J. Am. Chem. Soc. **103**, 3244 (1981).